most sensitive technique for detecting infectious DEN viruses (*16*). After 7 days, mosquito heads were examined by immunofluorescence for the presence of DEN-2 virus. Expression of D2prMa virus efficiently inhibited the biological transmission of DEN-2 virus because, of the 26 saliva samples tested, only one was weakly positive for DEN-2 infection (Table 1). In contrast, 20 of 26 saliva samples obtained from mosquitoes co-infected with TE/3′2J and DEN-2 viruses were positive for DEN-2 virus when inoculated into mosquitoes (Table 1). Saliva samples were scored positive for the presence of virus if at least one of the five saliva-injected mosquitoes was positive for DEN-2 antigen by immunofluorescence.

Both DEN-2–derived sense and antisense prM RNA have been shown to interfere with DEN-2 virus replication in mosquito cells. This interference is specific because there is no inhibition of replication of DEN-3 and DEN-4 viruses (*13*). Future work will focus on using dsSIN viruses to transduce mosquito cells with antisense RNAs that will target the genomes of all four DEN virus serotypes. The dsSIN transducing viruses are well suited for delivering anti-virus molecules to mosquito tissues where arbovirus replication occurs. These results show that antisense RNA can be used to ablate flavivirus transmission from *Aedes aegypti*. Ultimately, mosquito genomes will need to be manipulated with DNA-based transformation techniques to ensure both heritability and transcriptional control of the desired anti-virus agent in the mosquito (*21*).

REFERENCES AND NOTES

1. V. Deubel, R. M. Kinney, D. W. Trent, *Virology* **165**, 234 (1988). Y. S. Hahn *et al.*, *ibid.* **162**, 167 (1988).
2. T. J. Chambers, C. S. Hahn, R. Galler, C. M. Rice, *Annu. Rev. Microbiol.* **44**, 649 (1990).
3. S. B. Halstead, *Science* **239**, 476 (1988).
4. D. J. Gubler and D. W. Trent, *Infect. Agents Dis.* **2**, 383 (1993).
5. R. H. Whitehead, T. M. Yuill, D. J. Gould, P. Simasathien, *Trans. R. Soc. Trop. Med. Hyg.* **65**, 661 (1971); C. J. Leake, *Parasitol. Today* **8**, 123 (1992).
6. T. P. Monath, *Proc. Natl. Acad. Sci. U.S.A.* **91**, 2395 (1994).
7. J. C. Sanford and S. A. Johnston, *J. Theor. Biol.* **113**, 395 (1985). S. Higgs, A. Powers, K. Olson, *Parasitol. Today* **9**, 444 (1993).
8. A. M. Fallon, *Nature* **352**, 828 (1991).
9. C. S. Hahn, Y. S. Hahn, T. J. Braciale, C. M. Rice, *Proc. Natl. Acad. Sci. U.S.A.* **89**, 2679 (1992); K. E. Olson *et al.*, *Insect Biochem. Mol. Biol.* **24**, 39 (1994).
10. A. Rayms-Keller *et al.*, *Insect Mol. Biol.* **4**, 245 (1995); J. Carlson, K. Olson, S. Higgs, B. Beaty, *Annu. Rev. Entomol.* **40**, 359 (1995).
11. A. M. Powers, K. E. Olson, S. Higgs, J. O. Carlson, B. J. Beaty, *Virus Res.* **32**, 57 (1994).
12. A. M. Powers *et al.*, *Proc. Natl. Acad. Sci. U.S.A.*, in press.
13. P. J. Gaines *et al.*, *J. Virol.* **70**, 2132 (1996).
14. J. M. Murray, J. G. Aaskov, P. J. Wright, *J. Gen. Virol.* **74**, 175 (1993).
15. C6/36 cells were infected at a multiplicity of infection of 10 with the dsSIN viruses and incubated at 28°C for 48 hours. Total RNA was extracted by the acid guanidinium technique (*22*) from infected cells, fractionated on a formaldehyde denaturing gel (*23*), and transferred to a nylon membrane (Nytran Plus, Schleicher & Schuell, Keene, NH). An oligonucleotide probe (5′-gctggtcggatcattggggcg-3′) complementary to the dsSIN 3′ nontranslated region was end-labeled with [γ-^{32}P]deoxyadenosine triphosphate with the use of T4 polynucleotide kinase (Promega). The hybridization solution contained 10% dextran sulfate, 1% SDS, 4.8% NaCl (w/v), and 200 μg/ml of denatured salmon sperm DNA. The blot was hybridized at 50°C for 12 hours with 5×10^5 cpm of probe (specific activity $>10^8$ cpm/μg).
16. L. Rosen and D. Gubler, *Am. J. Trop. Med. Hyg.* **23**, 1153 (1974). *Aedes aegypti* mosquitoes originating from Rexville, Puerto Rico, were obtained from B. Miller, CDC Laboratory, Fort Collins, CO, and were reared at 28°C at 80% relative humidity and with a photoperiod of 16 hours of light and 8 hours of dark.
17. A. M. Powers and K. E. Olson, unpublished results.
18. B. J. Beaty and T. H. G. Aitken, *Mosq. News* **39**, 232 (1979). Immobilized mosquitoes were allowed to probe a 50-μl capillary tube filled with 15 μl of a solution containing 20% bovine fetal serum and 10% sucrose. Saliva was collected for 2 hours, at which time the mosquitoes were removed from the capillary tubes and the saliva transferred to a microfuge tube.
19. The dsSIN viruses in the saliva were neutralized with a mouse SIN polyclonal antibody (MB92) diluted 1:50. Viruses were neutralized for 1 hour at 4°C before each mosquito was intrathoracically injected with 0.5 μl of saliva.
20. Seven days after inoculating mosquitoes with saliva (*16*), we analyzed the mosquito heads for the presence of DEN-2 E antigen by indirect immunofluorescence assay using a DEN-2–specific mouse polyclonal antibody. The presence of DEN-2 antigen in the mosquitoes indicated the presence of DEN-2 virus in the saliva that escaped interference.
21. J. Crampton, A. Morris, G. Lycett, A. Warren, P. Eggleston, *Parasitol. Today* **6**, 31 (1990); N. J. Besansky and F. H. Collins, *ibid.* **8**, 186 (1992); M. Ashburner, *Science* **270**, 1941 (1995).
22. P. Chomczynski and N. Sacchi, *Anal. Biochem.* **162**, 156 (1987).
23. J. Sambrook, E. F. Fritsch, T. Maniatis, *Molecular Cloning: A Laboratory Manual* (Cold Spring Harbor Laboratory, Cold Spring Harbor, NY, ed. 2, 1989).
24. V. Deubel, R. M. Kinney, D. W. Trent, *Virology* **155**, 365 (1986).
25. D. Marchuk, M. Drumm, A. Saulino, F. S. Collins, *Nucleic Acids Res.* **19**, 1154 (1990).
26. C. M. Rice, R. Levis, J. H. Strauss, H. V. Huang, *J. Virol.* **61**, 3809 (1987).
27. G. Karber, *Arch. Exp. Pathol. Pharmakol.* **162**, 480 (1931).
28. A. C. Chanas, E. A. Gould, J. C. S. Clegg, G. R. Varma, *J. Gen. Virol.* **58**, 37 (1982).
29. E. A. Gould *et al.*, *ibid.* **66**, 1369 (1985).

30. We are indebted to C. M. Rice for generously providing the pTE/3′2J construct. This work was supported by the John D. and Catherine T. MacArthur Foundation and NIH grants AI34014 and AI07352.

15 January 1996; accepted 11 March 1996

Two Genetically Separable Steps in the Differentiation of Thymic Epithelium

Michael Nehls,* Bruno Kyewski, Martin Messerle,† Ralph Waldschütz, Kerstin Schüddekopf,‡ Andrew J. H. Smith,§ Thomas Boehm||

The development of the thymus depends initially on epithelial-mesenchymal and subsequently on reciprocal lympho-stromal interactions. The genetic steps governing development and differentiation of the thymic microenvironment are unknown. With the use of a targeted disruption of the *whn* gene, which recapitulates the phenotype of the athymic nude mouse, the WHN transcription factor was shown to be the product of the *nude* locus. Formation of the thymic epithelial primordium before the entry of lymphocyte progenitors did not require the activity of WHN. However, subsequent differentiation of primitive precursor cells into subcapsular, cortical, and medullary epithelial cells of the postnatal thymus did depend on activity of the *whn* gene. These results define the first genetically separable steps during thymic epithelial differentiation.

The primary function of the thymus is to generate and select a highly diverse repertoire of T cells that exhibit self tolerance and restriction to self major histocompatibility complex (*1*). The importance of the thymic microenvironment in shaping the T cell repertoire has long been recognized (*2*). Development of a functionally competent thymus depends on a series of epithelial-mesenchymal and subsequent lympho-stromal interactions (*3*), which implies the existence of developmentally restricted control points in the differentiation of thymic epithelium (*4*). Here, we have taken a genetic approach to identify the WHN transcription factor as an early regulator of thymic epithelial differentiation.

The *whn* gene (*5*) is mutated on mouse and rat nude alleles (*5*, *6*), which suggests that the WHN transcription factor is encoded by the *nude* locus. We used a targeted

M. Nehls, B. Kyewski, M. Messerle, R. Waldschütz, K. Schüddekopf, T. Boehm, Deutsches Krebsforschungszentrum, Im Neuenheimer Feld 280, 69120 Heidelberg, Germany.
A. J. H. Smith, MRC Laboratory of Molecular Biology, Hills Road, Cambridge CB2 2QH, UK.

*Present address: Zentrum der Inneren Medizin-Molekulare Kardiologie, Universität Frankfurt, 60590 Frankfurt, Germany.
†Present address: Institut für Virologie, Universität Heidelberg, Heidelberg, Germany.
‡Present address: Institut für Humangenetik, Universität Hamburg, 22529 Hamburg, Germany.
§Present address: Center of Genome Research, University of Edinburgh, Edinburgh EH9 3JQ, UK.
||To whom correspondence should be addressed. E-mail: t.boehm@dkfz-heidelberg.de

disruption of the *whn* gene, produced by homologous recombination in mouse embryonic stem cells, to verify this. In the original nude mouse allele, the third exon of the *whn* gene carries a single base pair deletion (*5*). For targeted inactivation of the *whn* gene, a Sfi I site in the third exon of the mouse *whn* gene close to the site of the spontaneous mutation (Fig. 1A) was used to insert a β-galactosidase (*lacZ*)-neo cassette (*7*).

Two independent, correctly targeted embryonic stem cell clones were used to establish mouse strains carrying the *whn* mutation, and mice heterozygous for the mutation ($whn^{+/-}$) were intercrossed to generate homozygous mutants ($whn^{-/-}$) (Fig. 1B). Both lines gave identical results: $whn^{-/-}$ animals exhibited all gross macroscopic features of the original nude mouse, such as hairlessness and athymia (Fig. 2). Flow cytometric analysis of lymphocytes isolated from spleen and mesenteric lymph nodes of 7-week-old mice revealed the complete absence of mature α/β T cells in −/− animals [as detected by antibodies to T cell receptor (TCR) β chain, CD4, and CD8], whereas +/− animals were indistinguishable from +/+ wild-type animals (Fig. 1C). The absolute frequency of B cells in −/− animals was unchanged in mesenteric lymph nodes and increased twofold in spleen as compared to +/+ and +/− mice. Similar findings have been described for nude mice (*8*).

When *nu/nu* mice were crossed with animals carrying the targeted insertion in the *whn* gene, no complementation of the characteristic pathologic features was observed in compound whn^{-}/nu heterozygotes, indicating that the two mutations are allelic. This result provides direct proof that the *whn* gene represents the *nude* gene (Fig. 2).

In the construct used for disruption of the *whn* exon 3, the β-galactosidase coding region is preceded by an internal ribosomal entry sequence (*9*); therefore, targeted insertion generates a bi-cistronic transcription unit (where two proteins are made from one mRNA) in which the expression of the gene encoding *Escherichia coli* β-galactosidase is under the control of *whn* transcriptional regulatory elements. The detection of the cytoplasmic reporter protein provides a distinct advantage over direct WHN protein detection, as WHN is a nuclear protein and thus not present in cytoplasmic extensions of the characteristic epithelial network in the thymus; furthermore, it provides a greatly improved resolution over RNA in situ hybridization analyses and facilitates co-localization studies with other proteins (*10*). At birth, the thymuses of $whn^{+/+}$ animals contain no β-galactosidase–positive cells and appear pale after in situ staining (Fig. 3A); in contrast, the thymuses of $whn^{+/-}$ animals are intensely blue (Fig. 3B). In $whn^{-/-}$ animals, no thymus can be detected; however, two cell aggregates located in the anterior mediastinum above the heart stain blue (Fig. 3C), indicating that the thymic rudiment in $whn^{-/-}$ animals contains β-galactosidase–positive cells.

To determine whether transcription of the *whn* locus begins before the immigration of lymphocyte precursors, we studied phenotypically normal heterozygous animals at embryonic day 12.5 (E12.5). β-Galactosidase activity was readily detected in two circumscribed regions of the pharyngeal region. At this stage, the thymic primordium (*11*) consists of two small clusters of epithelial cells positive for β-galactosidase, surrounded by a layer of flat mesenchymal cells with no evidence of lymphocytes (Fig. 3D). This finding suggests that *whn* expression occurs in the thymic primordium before the immigration of T cell precursors.

To determine whether sustained expression of *whn* requires the presence of functional WHN protein, the thymic rudiments of $whn^{-/-}$ mice were investigated. Even at birth, the alymphoid thymic rudiments of $whn^{-/-}$ mice [which at this stage consists of an encapsulated cystic aggregation of epithelial cells (*11*)] are positive for β-galactosidase (Fig. 3E), indicating that WHN

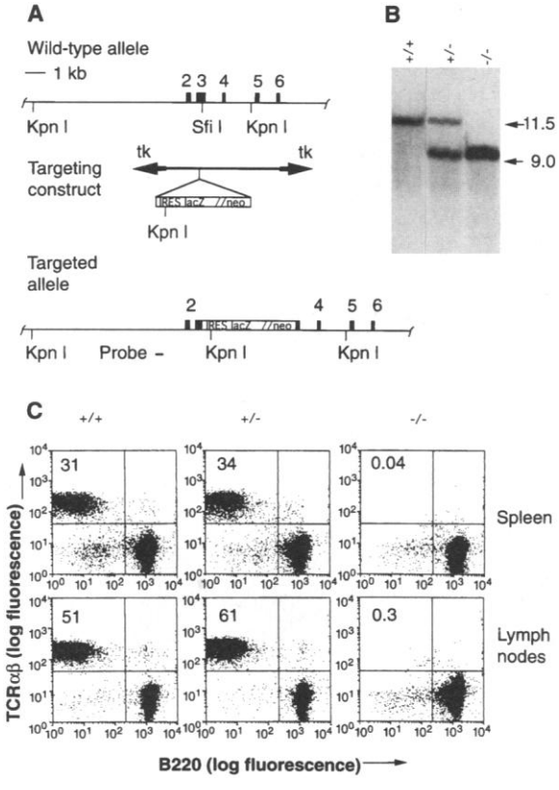

Fig. 1. Targeted mutation in *whn*. (**A**) Genomic structure (*17*) and targeting strategy. The wild-type allele with exons 2 to 6 is shown above the targeting construct (*18*); the structure of the targeted allele is shown below. Kpn I restriction sites in the relevant region of the gene are indicated. (**B**) Generation of homozygous mutant mice. Southern filter hybridization is shown with a 5′ flanking probe to Kpn I–digested genomic DNA isolated from animals of an intercross of $whn^{+/-}$ heterozygotes (*18*). Molecular size markers are shown on the right in kilobases. (**C**) $whn^{-/-}$ mice lack peripheral T cells. Mesenteric lymph node cells or splenocytes of $whn^{+/+}$, $whn^{+/-}$, and $whn^{-/-}$ mice were triple-stained (*19*) for expression of CD2, α/β TCR, and B220 (*20*). The relative expression of α/β TCR versus B220 on nucleated CD2-positive cells is shown. Note the normal distribution of α/β T cells and B cells in $whn^{+/-}$ mice and the complete absence of mature T cells in $whn^{-/-}$ mice; the percentage of α/β TCR–positive cells is given in the upper left quadrant.

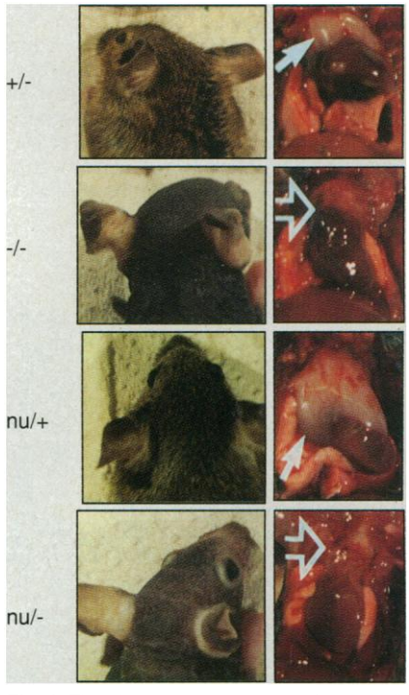

Fig. 2. The disrupted *whn* gene and *nu* are allelic. Mice carrying the original *nu* allele and mice carrying the targeted *whn* gene were crossed to yield all six possible genotypes, the four relevant of which are shown. The heads of animals (left) indicate the lack of hair growth in $whn^{-/-}$ and nu/whn^{-} animals; on the right, the thoracic situs are shown, indicating the absence of a normal thymus (open arrowhead) in $whn^{-/-}$ and nu/whn^{-} animals. Heterozygous animals (+/− and +/*nu*) are phenotypically normal; their thymuses are indicated by arrows.

does not regulate the activity of the *whn* promoter. It appears that a limited degree of proliferation of epithelial precursor cells can occur without lympho-epithelial interaction, as the number of cells in the thymic rudiments of $whn^{-/-}$ animals is greater than the number of cells found in the alymphoid thymic primordium.

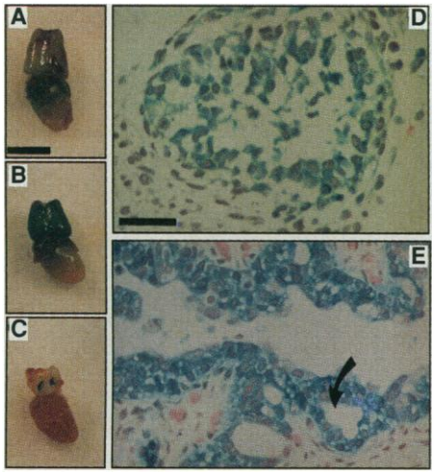

Fig. 3. Expression of the *whn* locus in thymus. Histochemical detection of β-galactosidase activity (*21*) was used as a measure for *whn* activity (see Fig. 1). (**A** through **C**) Hearts and thymuses from newborn mice were dissected and stained in situ. Note the absence of β-galactosidase activity in +/+ thymus (A), strong staining in +/− thymus (B), and intense staining of the thymic rudiment in −/− mice (C). (**D**) Alymphoid thymic anlage in a E12.5 +/− embryo (the day of finding the vaginal plug was taken as E1); all epithelial cells stain blue. (**E**) Alymphoid thymic rudiment in a newborn $whn^{-/-}$ animal. Note the cystic (arrow) appearance of the thymic rudiment consisting of blue epithelial cells. The scale bar in (A) applies also to (B) and (C) and represents 0.5 mm; the scale bar in (D) also applies to (E) and indicates 50 μm.

The expression of WHN in various subsets of thymic epithelia was studied in $whn^{+/-}$ animals. At birth, β-galactosidase activity is readily detectable in epithelial cells in the subcapsular region of the thymus, and positive cells are present throughout the cortical and medullary regions (Fig. 4). In thymuses from mice 7 weeks and 9 months of age, the epithelial cells from all regions of the thymus are still positive for β-galactosidase activity, although the pronounced expression in the subcapsular region is lost.

To substantiate the conclusion of generalized *whn* expression in thymic epithelial cells, we performed co-localization studies with keratin antibodies (anti-keratin). Keratin is a marker of thymic epithelial cells of all stages of differentiation (*12*). Using a cytokeratin antibody, we detected the typical immunofluorescence pattern of the thymic network in thymuses both at birth (Fig. 4) and in adults. Anti–β-galactosidase and anti-keratin staining patterns are virtually superimposable (Fig. 4A). Co-localization of β-galactosidase and ER-TR4 [a marker for cortical epithelial cells (*13*)] and ER-TR5 [a marker for medullary epithelial cells (*13*)] confirms expression of the *whn* gene in epithelial cells of both thymic compartments (Fig. 4B).

Several important conclusions can be drawn from these experiments. First, the WHN transcription factor (*5*) is the product of the *nude* locus. To confirm the circumstantial evidence (*5*, *6*), we provide here direct proof for the identity of the *nude* gene by the observation of the phenotype of athymic nude mice in whn^{-}/nu compound heterozygotes. Second, the initial formation of the thymic anlage does not require the activity of the *whn* gene because the alymphoid athymic rudiment becomes established in $whn^{+/+}$ and $whn^{-/-}$ mice. This suggests that *whn* acts downstream of a gene (or genes) specifying the development of the thymic primordium. Third, subsequent differentiation of thymic epithelial cells in the developing thymus strictly depends on a at least one wild-type copy of the *whn* gene. Because the expression of the *whn* gene begins before immigration of lymphoid precursors, the activity of *whn* is likely to be required for productive colonization of the thymic rudiment. Epithelial precursors of $whn^{-/-}$ mice may be frozen in an immature stage of differentiation; this result agrees with the finding of an abnormal surface phenotype of thymic epithelia in *nude* mice (*14*). However, because all major epithelial subsets in the thymus studied here continue to express *whn* throughout adult life, the activity of the WHN transcription factor may be required not only for the initiation but also for the maintenance of the differentiated phenotype of thymic epithelial cells.

Our results establish a genetically defined control point in thymic epithelial differentiation. The WHN transcription factor is required for progression beyond the alymphoid stage of the thymic rudiment. The identification of genes acting up- and downstream of *whn* will be required before the two steps now defined can be subdivided further.

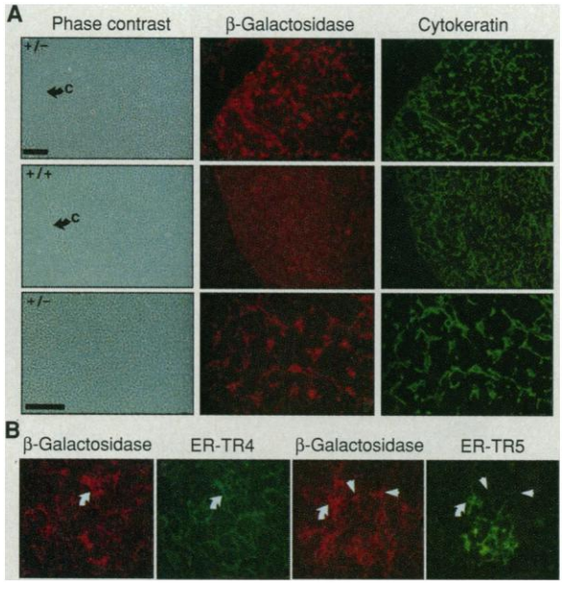

Fig. 4. Expression of β-galactosidase in subcapsular, cortical, and medullary thymic epithelial cells of $whn^{+/+}$ and $whn^{+/-}$ mice. Frozen sections of thymuses of newborn +/− and +/+ mice (**A**) or 3-week-old +/− mice (**B**) were double-stained for expression of β-galactosidase, cytokeratin (A), and ER-TR4 and ER-TR5 (B), respectively (*15*). In (A), β-galactosidase and cytokeratin expression patterns are superimposable. Note the relative abundance of β-galactosidase–positive cells in the subcapsular region of the newborn thymus. Subcapsular and outer cortical areas are shown; the capsule is indicated by an arrow in phase-contrast sections. No β-galactosidase staining above the background level was observed in +/+ thymuses. In (B), the distribution of ER-TR4, a marker of cortical epithelial cells, was similar to that of β-galactosidase (examples are highlighted by curved arrows), whereas ER-TR5, a marker of medullary epithelial cells, stained only a subset (arrowheads) of epithelial cells positive for β-galactosidase. The overall staining pattern of β-galactosidase–positive cells was more diffuse than that of cytokeratin or ER-TR antigens, which is consistent with the generalized cytoplasmic localization of β-galactosidase. Scale bars correspond to 50 μm.

REFERENCES AND NOTES

1. P. Kisielow and H. von Boehmer, *Adv. Immunol.* **58**, 87 (1995); S. C. Jameson, K. A. Hogquist, M. J. Bevan, *Annu. Rev. Immunol.* **13**, 93 (1995).
2. W. van Ewijk, *Annu. Rev. Immunol.* **9**, 591 (1991); M. A. Ritter and R. L. Boyd, *Immunol. Today* **14**, 462 (1993).
3. R. Auerbach, *Dev. Biol.* **2**, 271 (1960); N. M. Le Douarin, F. Dieterlen-Lièvre, P. D. Oliver, *Am. J. Anat.* **170**, 261 (1984); G. Anderson, E. J. Jenkinson, N. C. Moore, J. J. T. Owen, *Nature* **362**, 70 (1993); W. van Ewijk, E. W. Shores, A. Singer, *Immunol. Today* **15**, 214 (1994).
4. E. W. Shores, W. van Ewijk, A. Singer, *Eur. J. Immunol.* **21**, 1657 (1991); G. A. Holländer *et al.*, *Nature* **373**, 350 (1995).
5. M. Nehls *et al.*, *Nature* **372**, 103 (1994).
6. J. A. Segré *et al.*, *Genomics* **28**, 549 (1995).
7. A. J. H. Smith *et al.*, in preparation.
8. H. R. MacDonald *et al.*, *J. Immunol.* **126**, 885 (1981); K. Kishihara *et al.*, *Eur. J. Immunol.* **17**, 477 (1987); B. E. Rich and P. Leder, *J. Exp. Med.* **181**, 1223 (1995).
9. P. Mountford *et al.*, *Proc. Natl. Acad. Sci. U.S.A.* **91**, 4303 (1994).
10. β-Galactosidase activity correlates with the transcriptional activity of the targeted gene (*9*); because no endogenous β-galactosidase activity can be detected in wild-type thymuses at all stages of devel-

opment, *whn* gene expression during thymic development was characterized throughout with the β-galactosidase reporter protein.
11. A. C. Cordier and S. M. Haumont, *Am. J. Anat.* **157**, 227 (1980).
12. A. J. Laster, T. Itoh, T. J. Palker, B. F. Haynes, *Differentiation* **31**, 67 (1986).
13. E. van Vliet, M. Melis, W. van Ewijk, *Eur. J. Immunol.* **14**, 524 (1984).
14. E. van Vliet *et al.*, *ibid* **15**, 675 (1985).
15. P. Altevogt, M. Michaelis, B. Kyewski, *ibid.* **19**, 1509 (1989).
16. Tissues were dissected out and fixed for 2 hours on ice in phosphate-buffered saline (PBS), 1% formaldehyde, 0.2% glutaraldehyde, 0.02% NP-40, and 1 mM $MgCl_2$, washed twice in PBS and 0.05% bovine serum albumin, and then stained overnight at 37°C in PBS and 1 mM $MgCl_2$, 0.04% X-Gal, 5 mM potassium ferrocyanide, and 5 mM ferricyanide. Tissues were then washed, post-fixed in PBS and 4% paraformaldehyde, and processed for histological analysis. Sections were counterstained with eosin and hematoxylin.
17. The complete genomic structure of the mouse *whn* locus will be described (M. Schorpp *et al.*, in preparation).
18. The targeting construct was derived as follows. P1 recombinants spanning the *whn* locus [M. Nehls *et al.*, *Mamm. Genome* **6**, 321 (1995)] were partially digested with Sau 3AI, selected by size, and cloned into λKO [M. Nehls, M. Messerle, A. Sirulnik, A. J. H. Smith, T. Boehm, *Biotechniques* **17**, 770 (1994)], which supplies thymidine kinase genes at either end of the insert. Recombinants containing exon 3 were analyzed for inserts in which the Sfi I site was at a reasonable distance from one end of the insert, to facilitate subsequent polymerase chain reaction (PCR) screening. In the clone used here (32), the Sfi I site was located about 1.8 kb downstream of the 5′ end of the homologous sequences and about 4.2 kb upstream of the 3′ end of the homologous sequences. Phage DNA was concatamerized by ligation at its cos ends and then cut with Sfi I. The Sfi I ends were modified by addition of Bam HI adapter oligonucleotides and this DNA subsequently ligated to a Bam HI cassette containing a promoterless β-galactosidase gene preceded by an internal ribosomal entry sequence followed by a neomycin resistance gene (7). The ligation was packaged in vitro, and desired recombinants were selected by plaque hybridization, converted into plasmid form, and linearized with Not I. This linear molecule was then ligated to a self-complementary Not I–compatible, phosphorylated oligonucleotide (5′-GGCCTCCGGTACATGATCGAGGGGACTGACAAGACGGCCAGTCCTCGATCATGTACCGGA-3′) to seal the ends of the linear fragment. This treatment enhances the stability of transfected DNA, improves positive-negative selection, and increases the frequency of homologous recombination (M. Messerle and T. Boehm, in preparation). The targeting construct was transfected into CJ7 cells [P. J. Swiatek and T. Gridley, *Genes Dev.* **7**, 2071 (1993)], and clones resistant to G418 and gancyclovir were analyzed by PCR and Southern (DNA) blotting for homologous recombination. Of 25 colonies tested, 23 were homologous integrants. Mice heterozygous for the insertional mutation were derived as described [A. Warren *et al.*, *Cell* **15**, 45 (1994)].
19. For flow cytometric analysis, cell suspensions of mesenteric lymph nodes and spleen were depleted of erythrocytes by brief NH_4Cl treatment and then triple stained with the following antibody combinations: antibodies to α/β TCR–fluorescein isothiocyanate (FITC) (*15*), CD4-phycoerythrin (PE), CD8–Red 613 (both from Gibco-BRL), or α/β TCR-FITC, B220-PE (Pharmingen, San Diego), and CD2-biotin (*16*)–streptavidin–Red 670 (Gibco-BRL). Cells were analyzed with a FACScan cytometer (Becton and Dickinson, Heidelberg, FRG). Lymphoid cells were gated by appropriate forward and side scatter, and 10,000 events were analyzed with Lysis-II software. The cell yield from $whn^{+/+}$, $whn^{+/-}$, and $whn^{-/-}$ mice was 1.2×10^7, 0.7×10^7, and 0.4×10^7 for mesenteric lymph nodes, and 4.6×10^7, 4.0×10^7, and 6.0×10^7 for splenocytes, respectively. The frequency of CD2-positive cells ranged between 93 to 99% but was reduced to 65% in spleen cells of $whn^{-/-}$ mice, indicating an increase of nonlymphoid cells.
20. R. T. Kubo *et al.*, *J. Immunol.* **142**, 2736 (1989).
21. Frozen sections (3 μm) were acetone-fixed, pretreated with human γ globulin (Venimmun, Behringwerke AG, Marburg, FRG), and stained with the following antibody combinations: (i) rabbit immunoglobulin G (IgG) anti–β-galactosidase (Organon Teknika, West Chester, PA), goat antibody to rabbit IgG-Cy3 (Jackson, Avondale, PA) supplemented with 5% normal goat serum, mouse antibody to pan-cytokeratin (clone Lu-5, Dianova GmbH, Hamburg, FRG), and goat antibody to mouse IgG1-FITC (Southern Biotechnology Association, Birmingham, AL); (ii) rabbit-IgG anti–β-galactosidase, goat antibody to rabbit IgG-Cy3 supplemented with 5% normal goat serum, ER-TR4 (*13*) or ERTR5 (*13*) culture supernatant, $F(ab')_2$ goat antibody to rat IgG-biotin (Jackson) supplemented with normal goat and rabbit sera at 5% each, and streptavidin-FITC (Boehringer Mannheim, FRG). Stained sections were photographed with an Axiophot microscope (Zeiss) with Fujichrome Provia 400 film.
22. We thank T. H. Rabbitts for advice, I. Schuster, S. Höflinger, G. King, and T. Langford for expert technical help, H. Schrewe for CJ7 cells, and W. van Ewijk for antibodies. These studies were supported by a grant from the Deutsche Forschungsgemeinschaft (Bo1128/2-2). A.J.H.S. is supported by the Association of International Cancer Research.

31 January 1996; accepted 25 March 1996

Chemical Usurpation of a Nest by Paper Wasp Parasites

Anne-Geneviève Bagnères,* Maria Cristina Lorenzi, Georges Dusticier, Stefano Turillazzi, Jean-Luc Clément

The paper wasp *Polistes atrimandibularis* is an obligatory social parasite of another *Polistes* species, *P. biglumis bimaculatus*. To control the host nest, the parasite sequentially changes the composition of its chemical signature, the cuticular hydrocarbons, during the colonial cycle. Gas chromatography–mass spectrometry of the cuticular hydrocarbons at every stage of the cycle showed that the parasite can switch on and off an entire chemical family, namely, the unsaturated hydrocarbons. In this way the parasite can match the host signature at a critical moment of the colonial cycle.

Having no worker caste and being incapable of nest building, *P. atrimandibularis* is an obligatory social parasite. During the short 4-month summer colonial cycle of the host, a *P. atrimandibularis* queen usurps a nest of a *P. biglumis bimaculatus* foundress (*1*, *2*). Nest invasion occurs within the span of a few hours, during which the initially unaggressive parasite becomes increasingly dominant and begins egg laying. In contrast the host queen, at first very aggressive, becomes subdued (*3*). To date there has been no satisfactory explanation for the ease with which *P. atrimandibularis* controls the host colony.

In insects, environmental perception often relies heavily on olfaction, gustation, or both. In social wasps, nestmate–non-nestmate discrimination depends on odors (*4*). These findings led us to suspect that chemical mimicry could be involved in nest usurpation by *P. atrimandibularis*. Like other social insects, the host *P. biglumis bimaculatus* has a chemical signature that facilitates recognition between colony members (*5*). This species- and colony-specific signature depends mainly on cuticular hydrocarbon components (*6*), which are dependent on environmental and physiological factors (*7*). Plasticity or camouflage of cuticular hydrocarbon patterns has already been reported in insects living in natural and artificial heterospecific colonies (*8*).

The purpose of this study was to better understand the integration mechanism by comparing the chemical signature of the parasite, the host, and their descendants collected in the field at different times of the colonial cycle. We extracted almost 80 different cuticular products from the two species, all of which were hydrocarbons ranging in chain length from C_{23} to C_{37}. Data for mathematical and statistical analysis were obtained by gas chromatography (GC) on individual extracts, and the identification of hydrocarbons was achieved by GC–mass spectrometry (GC-MS) on pooled extracts (*9*). Considerable variations in cuticular hydrocarbons of individuals were noted during the short colonial cycle (*10*).

Polistes atrimandibularis queens, fertilized in the previous summer, begin searching for a host comb about 1 month after solitary nest founding in early June by the host queen. At this time, just before invasion (late June), the cuticular signatures of the two species are distinct (Fig. 1A). The signature of *P. atrimandibularis* females is extremely rich in unsaturated hydrocarbons,

A.-G. Bagnères, G. Dusticier, J.-L. Clément, CNRS UPR 9024, Laboratoire de Neurobiologie-Communication Chimique, 31, Chemin Joseph Aiguier, 13402 Marseille Cedex 09, France.
M.-C. Lorenzi, Dipartmento di Morfofisiol Veterinaria, Università di Torino, Viale Mattioli 25, 10125 Turin, Italy.
S. Turillazzi, Dipartmento di Biologia Animale é Genetica, Università di Firenze, Via Romana 17, 50125 Florence, Italy.
*To whom correspondence should be adressed.